P5B.5 RELATION BETWEEN SUBSEASONAL AND INTERANNUAL VARIABILITY OF INDIAN MONSOON AND POTENTIAL FOR SEASONAL PREDICTABILITY IN A COUPLED GCM

Deepthi Achuthavarier*[1] and V. Krishnamurthy[1,2]
[1]Department of Climate Dynamics, George Mason University, Fairfax, Virginia
[2]Center for Ocean-Land-Atmosphere Studies, IGES, Calverton, Maryland

1. INTRODUCTION

The observed record of rainfall over India shows that the Indian summer monsoon experiences significant interannual variability in the seasonal [June-July-August-September (JJAS)] mean rainfall. The summer monsoon also exhibits subseasonal oscillations of periods 45-day and 20-day, the combined effects of which contribute to the active and break cycles (Krishnamurthy and Shukla 2006a, KS06a hereafter). Using numerical models, Charney and Shukla (1981) showed that the seasonal variability in the tropics is largely influenced by the atmospheric boundary conditions such as sea surface temperature (SST), snow cover, soil moisture rather than the atmospheric internal dynamics. This finding suggests that there is hope for seasonal prediction of the monsoon, provided the boundary anomalies are predictable and their relation with the rainfall is well understood.

Despite the fact that there is potential for prediction, dynamical seasonal prediction of monsoon rainfall still remains a challenging problem. Krishnamurthy and Shukla (2000) (KS00 hereafter) suggested a modified Charney-Shukla hypothesis and proposed a conceptual model to explain the interannual variability of the seasonal mean monsoon. According to their model, the seasonal mean precipitation consists of an externally forced large-scale seasonally persistent component and a subseasonal component that may be independent of external forcings. The relative strength of these components determines the seasonal mean. Using observed rainfall data, KS00 showed that the interannual variability of monsoon is not fully explained by the frequency and extent of the individual active and break cycles and hence suggests the presence of seasonally persistent components. Multi-channel Singular Spectrum Analysis (MSSA) of observed rainfall and outgoing longwave radiation (OLR) data confirms the presence of seasonally persisting components and their influence on interannual variability (Krishnamurthy and Shukla 2006a; 2006b (KS06b hereafter)).

This paper is an extension of the observational studies of KS00, KS06a and KS06b to a coupled General Circulation Model (GCM). The potential for operational seasonal forecasts in the monsoon region is closely tied to the ability of a GCM to generate seasonally persistent components that are both correct in amplitude and in their correlations with boundary conditions. The Climate Forecast System (CFS), the latest coupled GCM developed by the National Centers for Environmental Prediction (NCEP) is chosen for this study. The objective of this study is to find whether the GCM produces seasonally persistent and subseasonal signals during the summer monsoon season as seen in observational analysis by KS00 and KS06a. The influence of the seasonally persistent signals on the interanual variability and its correlation with SST are also examined.

A brief description of the CFS model and data analysis methods are provided in section 2. Using composite and pattern correlation analyses, the role of active and break phases in determining the seasonal mean monsoon is examined in section 3. In section 4, the seasonally persisting and subseasonal oscillatory modes are determined using MSSA. The relation between persisting modes and SST is examined in section 5. Section 6 provides summary and discussions.

2. MODEL AND ANALYSIS METHODS

2.1 Model

The CFS is a fully coupled GCM developed by the NCEP and is currently being used for operational dynamical seasonal prediction. The atmospheric component of this model is the Global Forecast System (GFS) and the ocean component is the Modular Ocean Model version 3 (MOM3) by Geophysical Fluid Dynamics Laboratory (GFDL). The CFS has a spectral triangular truncation of 62 waves in the horizontal and a finite differencing in the vertical with 64 sigma layers. The ocean

* *Corresponding author address:* Deepthi Achuthavarier, Department of Climate Dynamics, George Mason University, Fairfax, VA 22030; e-mail: deepthi@cola.iges.org.

component uses spherical coordinates in the horizontal and z coordinate in the vertical. The zonal resolution is 1° and the meridional resolution is 1/3° between 10°S and 10°N and increases through tropics and becomes fixed at 1° degree poleward of 30°S and 30°N. There are 40 layers in the vertical. The atmosphere-ocean coupling in CFS spans from 65°S to 50°N. The CFS is a fully coupled system with no flux correction. The atmosphere and ocean components exchange daily averages of heat and momentum fluxes once a day. A detailed description of the model can be found in Saha et al. (2006).

2.2 Analysis Methods

Daily data of precipitation, OLR and SST for a period of 30 years (1991-2020) were obtained from a long control run of the CFS (K. Pegion, Personal communication). The composite and spatial pattern correlation analyses performed in section 3 require proper separation of daily and seasonal anomalies. We follow the procedure outlined by KS00 in defining the seasonal and daily anomalies. Seasonal anomalies are calculated by subtracting the seasonal climatology from the seasonal means. Similarly, daily anomalies are calculated by subtracting the daily climatology from the daily means. As the daily anomalies in this case include the seasonal anomalies, the daily anomalies are then redefined by subtracting the seasonal anomalies from them. Thus the daily anomalies of rainfall referred in section 3 do not contain seasonal anomalies. Additionally, small-scale fluctuations in the daily data are removed by applying a 5-day running mean. The daily anomalies and means of rainfall and OLR mentioned hereafter are 5-day running means unless specified otherwise.

In section 4, Multi channel Singular Spectrum Analysis (MSSA) is applied on daily anomalies of OLR to determine seasonally persisting and subseasonal signals. While a traditional empirical orthogonal function (EOF) analysis provides the spatial patterns of maximum variance, MSSA isolates the spatial structure of the most dominant modes as well as their propagation in time (Plaut and Vautard, 1994). In the context of a dynamical system, MSSA can be considered as a tool to isolate quasi-periodic and quasi- stationary orbits of the system. MSSA has been used to study intraseasonal variability in the midlatitudes by Plaut and Vautard (1994) and in the tropics by KS06a and KS06b. The computational procedure of MSSA can be briefly described as follows. Let the original data set contain L spatial points (channels) at N discrete time intervals. The lagged covariance matrices are constructed by choosing a certain lag window of length M for each L spatial point. The lagged covariance matrices for all spatial points are arranged to form a trajectory matrix of order (LM, (N-M+1)), eigen analysis of which yields LM eigenvalues and LM eigenvectors. The eigenvectors contain M sequence of spatial maps and are referred as space-time EOFs (ST-EOFs). The space-time principal components (ST-PCs) each of length N-M+1 are found by projecting the original data on to the corresponding ST-EOFs. The component of the original data corresponding to each eigenvalue can be constructed by projecting the ST-PC onto its respective ST-EOF, and thus MSSA provides a data adaptive filtering method, and is referred to as the reconstructed component (RC). A detailed description of the mathematical formulation of MSSA can be found in Plaut and Vautard (1994) and Ghil et al. (2002).

3. SPATIAL STRUCTURE OF VARIABILITY

Preliminary analyses (figures not shown) suggest that the CFS simulates the Indian monsoon climatology and variability reasonably well. The spatial structure of the standard deviation of seasonal anomaly of precipitation appears to have good correspondence with that of observations although the amplitude of variability is generally greater by 1 to 1.5 mm day^{-1} in the model. The standard deviation of the daily anomalies compare well with observations over the southwestern parts of the country although it is largely underestimated over central India.

The objective of the analysis in this section is to examine whether the frequency of active and break cycles of the summer monsoon contribute significantly toward the seasonal mean. Palmer (1994) proposed that the seasonal mean rainfall of a year is an aggregate of the individual active and break cycles occurred in that year. This suggests that whether a seasonal mean is above or below normal is determined only by the frequency and extent of the active and break cycles occurring during that year. Additionally, this suggests that the spatial patterns of seasonal and daily variance should resemble each other. This concept was tested using a long record of observed rainfall by KS00 and was shown that the spatial structure of daily and seasonal variance are distinct and it was unlikely that the interannual variability is explained only by the individual active and break cycles.

First, we examine the spatial structure of the subseasonal and the interannual variability by computing composites of active and break periods

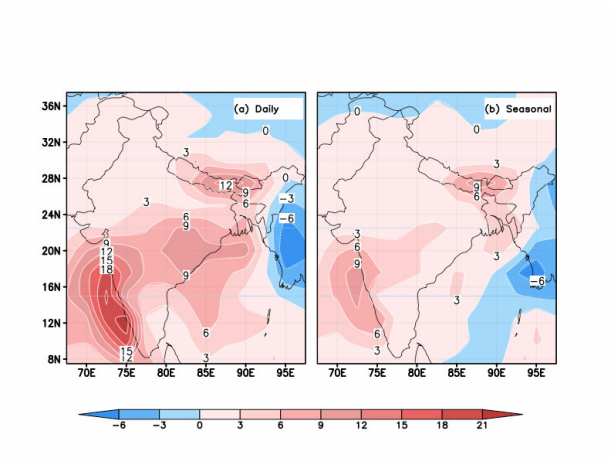

Figure 1. Difference between active and break composites of daily rainfall anomalies (a) and difference between strong and weak composites of JJAS seasonal anomalies (b) during the period 1991-2020. The rainfall is in mm day^{-1}. Daily anomalies are 5-day running means.

and strong and weak monsoon seasons. The active and break phases and the strong and weak seasons are defined according to KS00. A period is considered active (break) when the standard deviation of the daily anomalies of the IMR (area averaged rainfall over the Indian land region) index stands above (below) + (-) 0.5 units for at least 5 consecutive days. Similarly, a monsoon year is categorized as strong (weak) when the standard deviation of the seasonal anomalies of the IMR index is above (below) + (-) one unit. Based on this, we obtained 4 strong monsoon years (1991, 2004, 2009, 2010) and 3 weak monsoon years (1992, 1993, 2013). The criterion on the daily anomalies gave 815 active days and 1047 break days during the period 1991-2020. The active and break composites are computed by averaging the actual daily anomalies (that do not include seasonal anomalies) during the JJAS season from 1991 to 2020. Similarly, the actual seasonal anomalies are averaged to obtain the strong and weak year composites. The difference between the active and break composites and strong and weak year composites are shown in Figure 1. Both the seasonal and daily patterns have somewhat similar structure, such as the maxima along the west coast, over the eastern parts of the central India and over the northeastern regions. However the seasonal composite has a more uniform pattern over the entire region, and the local minima over the northeast and southeast are not as dominant as they appear in the daily anomalies. Similar analysis using observed data shows striking difference between the seasonal and daily composites (see KS00). The seasonal composite has a large scale structure covering the entire Indian land mass while the daily composite is characterized by same sign anomalies over the southwest and central India and opposite sign anomalies over the southeast and northeastern parts of the country. Although the model shows some indication of reduced rainfall over the south eastern (east of 77°E and between 8°N and 16°N) and north eastern (east of 76°E and between 26°N and 28°N) regions, in general, it fails to reproduce the spatial features associated with the active and break periods.

Secondly, we examine the pattern correlation between the seasonal anomalies and daily anomalies that include the seasonal anomalies as well as the daily anomalies that do not include the seasonal anomalies. Both the seasonal anomalies and the daily anomalies are standardized by their respective standard deviations. Figure 2 shows the pattern correlations for three selected years where monsoon is strong, weak or normal. The correlation is consistently positive when the seasonal anomalies are included in the daily anomalies, but it oscillates between positive and negative values when seasonal anomalies are removed. This behavior is observed in all the 30 years studied. According to the hypothesis by Palmer (1994), pattern correlations during a flood year are expected to be generally positive and those during a drought year negative. However Figure 2 does not show any such bias during strong or weak years. The positive correlation values obtained when the daily anomalies include seasonal anomalies suggest that a seasonally persistent component of the rainfall exists. These results support the conceptual model by KS00 and suggest that the frequency of active and break cycles are indistinguishable between strong and weak monsoon years.

4. MSSA OF OLR

The space-time structure of individual modes of variability are obtained by applying MSSA on 5-day running means of daily anomalies of OLR over the south Asian monsoon region (40°E-160°E, 35°S-35°N). The analysis is restricted to JJAS season (122 days) during the 30 years of the model run. The rainfall over India during pre-monsoon and post-monsoon periods can be often as small as zero and hence an analysis using the

daily data for the whole year is difficult. Using a lag window length (M) of 61 days, we obtain ST-PCs of length 62 days and ST-EOFs each of which consists of a sequence of 61 maps. The original data that correspond to the leading eigenmodes are reconstructed by projecting the ST-EOFs on to their respective ST-PCs. The reconstructed

of the power spectrum of the ST-PCs of the first 8 eigenmodes (figure not shown) suggests that the modes 1, 3 and 4 are clearly seasonally persisting signals while 6 and 7 constitute an oscillatory pair. The period of oscillation of the pair 6-7 is about 30 days and appears to be the equivalent of the 28-day oscillation obtained from the observational

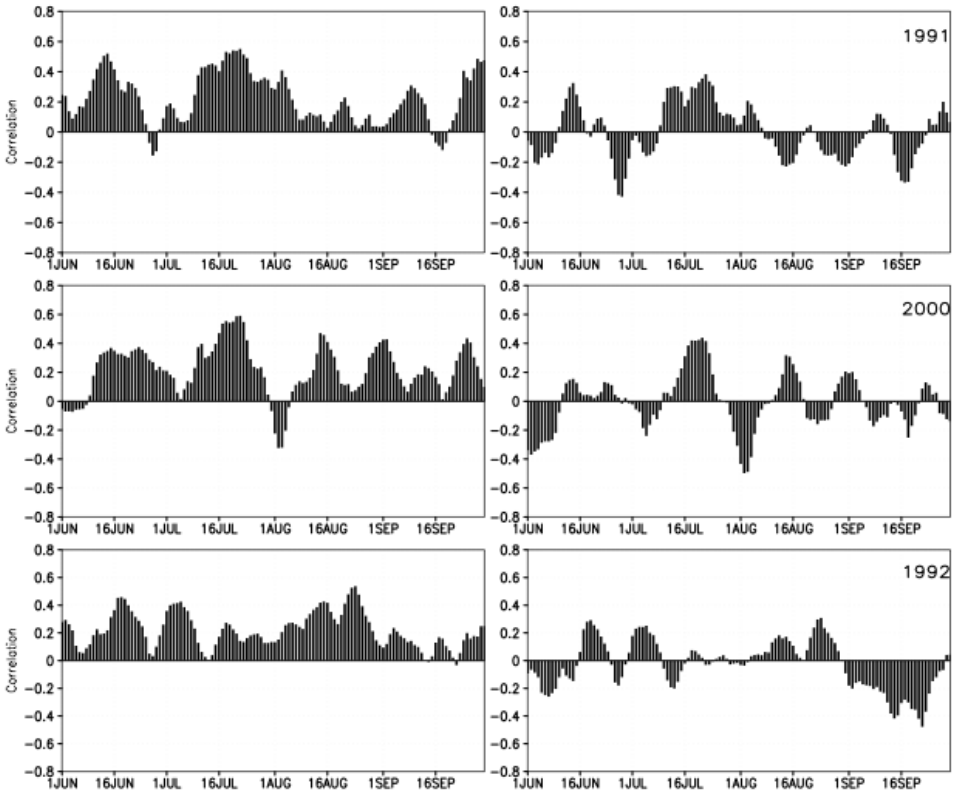

Figure 2. Spatial pattern correlation between standardized daily anomalies that include seasonal anomalies and standardized seasonal anomalies for a strong year (1991), normal year (2000) and a weak year (1992) (left panel). Spatial pattern correlation between standardized daily anomalies that does not include seasonal anomalies and standardized seasonal anomalies for a strong year (1991), normal year (2000) and a weak year (1992) (right panel).

components (RCs) are spatial patterns of individual eigenmodes corresponding to each day in the original time series.

The fraction of the total variance explained by the first 8 eigenvalues is about 17.2%, and these eigenmodes are considered to be the dominant modes of variability in the model. An examination

data by KS06a. The power spectra of the ST-PCs 2 and 5 have distinct peaks between 45 and 120 days and therefore cannot be considered as persisting components. These modes are not oscillatory pairs either since their eigenvalues do not occur in pair. The ST-PC 8 has a small peak around 80 days.

In order to understand the spatial structure of variability, the RCs for the first 8 eigenmodes were computed and their spatial EOFs are examined in Figure 3. MSSA of observed OLR data over the same region shows the presence of two seasonally persistent signals with distinct spatial features (KS06b). One of the persistent components has same sign of anomalies over

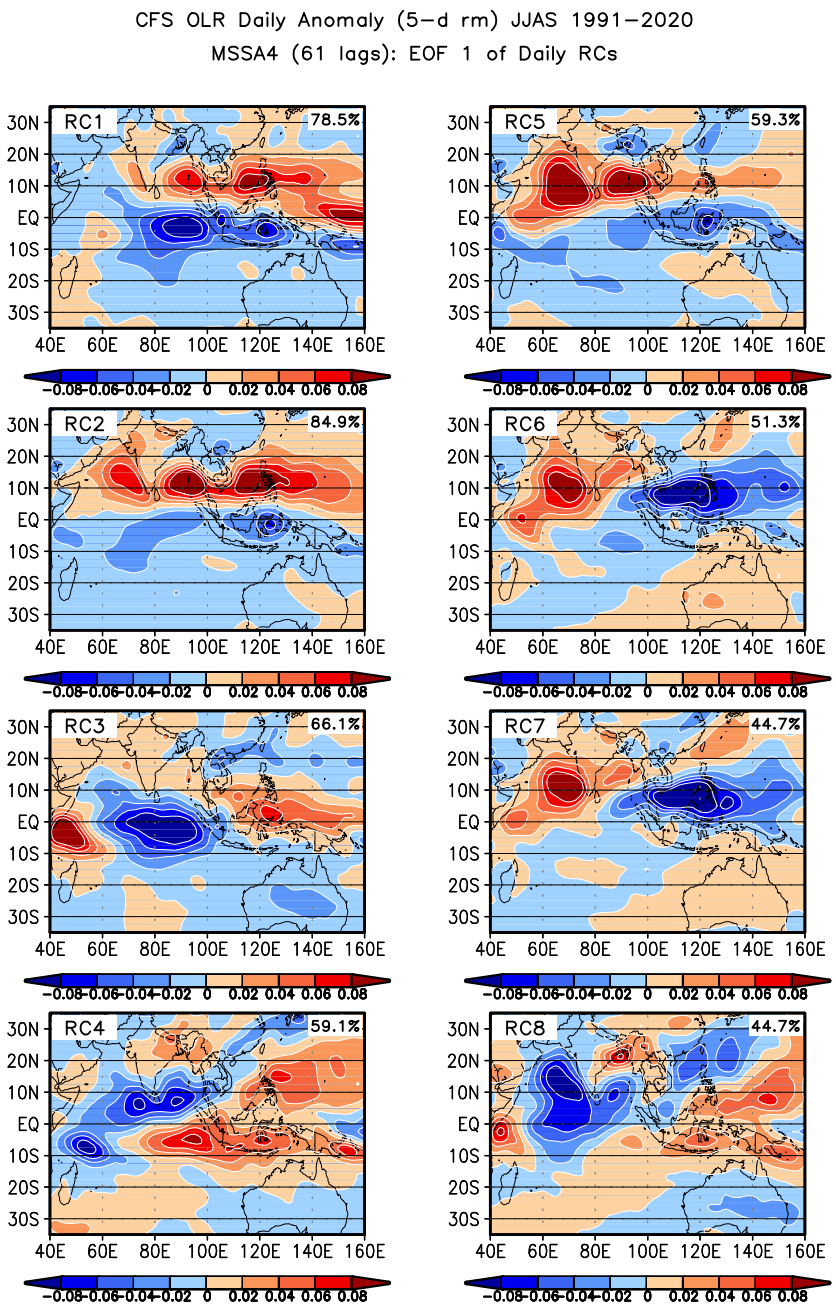

Figure 3. First spatial EOFs of the reconstructed components (RCs 1 to 8) of daily anomalies of OLR. The percentage variance explained by EOFs are given on the top right corner. Units are arbitrary.

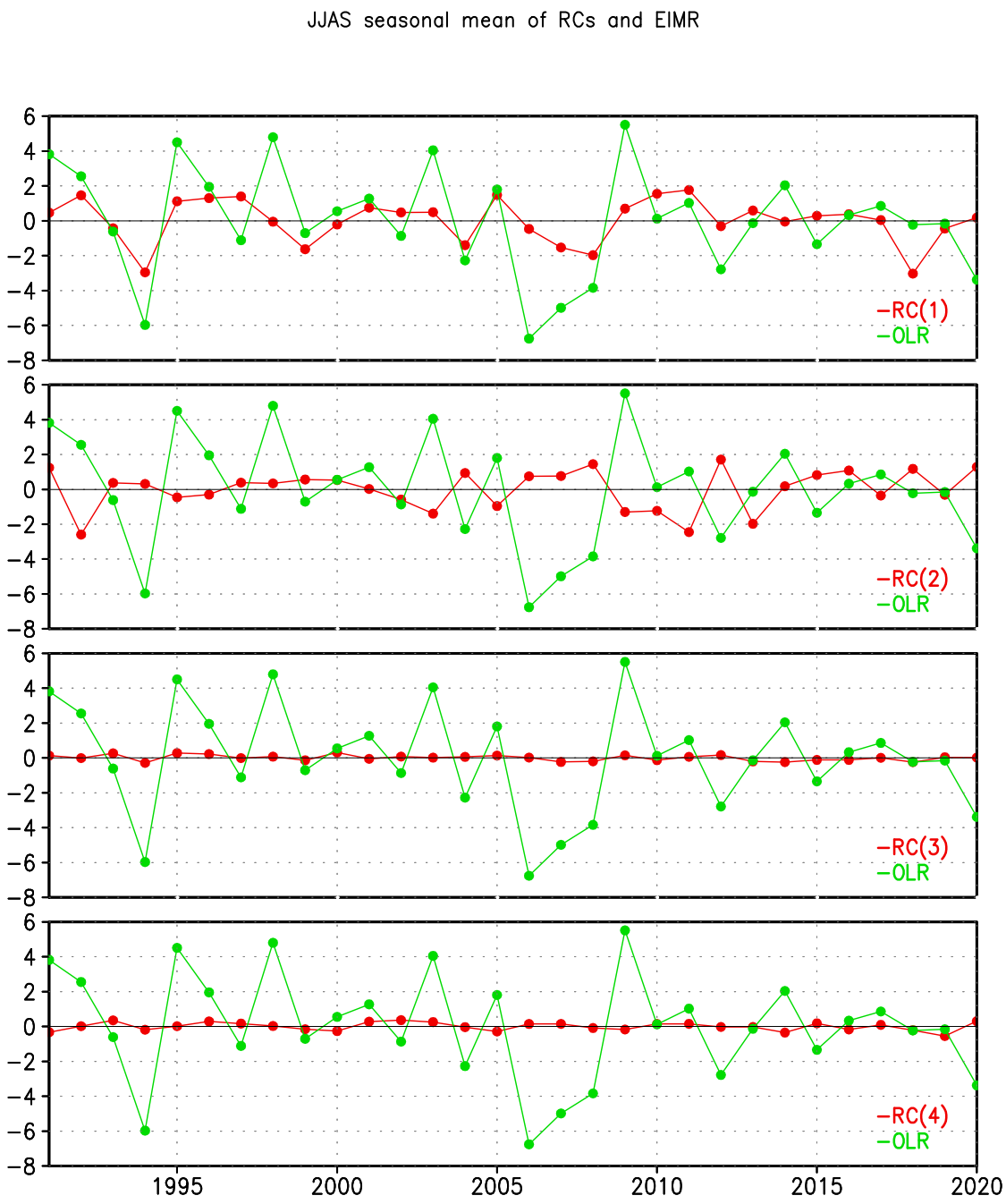

Figure 4. JJAS seasonal mean of the reconstructed components (RCs 1 to 4) and total OLR anomaly averaged over the EIMR region (Wm^{-2}). Both total OLR and RCs are multiplied by -1.

most of the monsoon region (40°E-140°E, 20°S-30°N) and opposite sign of anomalies over a small region east of 140°E. The second persistent component has a dipole structure in the Indian Ocean with opposite signs of anomalies on either side of the 80°E line. The objective here is to examine if any of the persisting signals found in the model correspond to either of these modes obtained from observations.

Figure 3 shows the first EOFs of the RCs 1 to 8 obatined from a new spatial EOF analysis of the RCs. It can be seen that RC-1 has a spatial structure with positive anomalies extending over most of the region north of 5°N and negative

anomalies over south of 5°N. The spatial uniformity in this structure suggests a large-scale influence on the rainfall over the region. RC-3, which is also resolved as a persistent signal, shows a clear dipole-like pattern in the equatorial Indian Ocean. Positive anomalies extend over most of the Indian land region and maritime continents with a peak over the west coast of Africa and negative anomalies extend over the rest of the region with a peak over the Indian Ocean between 10°S and 8°N. This pattern appears to have good correspondence with the dipole structure found in observations by KS06b. Another clear persistent signal, RC-4, has positive anomalies over much of the southern Indian Ocean, the maritime continent, the western Pacific and over the north eastern parts of the Indian subcontinent. Negative anomalies are found over the west coast of Africa and on either side of the Indian peninsula. The spatial pattern of RC-8 has some similarity with that of RC-4, especially in the structure and extent of positive anomalies over the southern Indian Ocean and maritime continent and the negative anomalies over the Indian peninsular region. However RC-8 has positive anomalies over the west coast of Africa which is not seen in RC-4. RCs 6 and 7 are oscillatory pairs, and their individual spatial patterns are similar. The propagation characteristics of RCs 6 and 7 that cannot be revealed by spatial EOFs are best understood by constructing phase composites or frequency-wave number spectra. A phase composite analysis of RCs 6 and 7 did not show good correspondence with the propagation characteristics of the 28-day mode obtained by KS06a. Further analyses are being carried out to understand the nature of this oscillatory pair. Although not resolved as an oscillatory pair, RCs 2 and 5 appear to have similar spatial structures (signs of EOF are arbitrary). Positive anomalies are seen over most of the Indian land region and over the Bay of Bengal and western Pacific in RC-2 while mostly negative anomalies are seen over these regions in RC-5. Similarly most of the regions south of the equator have negative anomalies in RC-2 and positive anomalies in RC-5.

In order to see the influence of each of the RCs in deciding the interannual variability of rainfall, the seasonal mean of RCs 1 to 4 are compared with the total seasonal anomalies of OLR. Seasonal mean RCs and total seasonal anomalies of OLR are computed and averaged over the Extended Indian Monsoon Rainfall (EIMR) region. The EIMR region extends from 70°E to 110°E in longitude and 10°N to 30°N in latitude covering the Indian land area as well as the adjacent oceanic region (Goswami, et al. 1999). The EIMR indices for the RCs and total OLR anomalies are shown in Figure 4. Both indices are multiplied by -1 for easy comparison with rainfall. It can be seen that RC-1 is the component that captures some amount of the interannual variability produced by the model. RCs 3 and 4 have very little variability from year to year. RCs 5 to 8 were also found to have insignificant interannual variability, figures of which are not shown here. A reasonably well correspondence seen between the persistent component RC-1 and seasonal anomalies of OLR is in agreement with the conceptual model proposed by KS00 and results from observations by KS06a.

5. RELATION BETWEEN PERSISTENT MODES AND SST

In order to investigate whether the persistent modes are influenced by the boundary conditions, the correlation between RCs and SST is computed in this section. Point correlation between PC-1 from the spatial EOF analyses of the first 8 RCs and JJAS daily anomalies of SST over the entire tropics (30°S to 30°N) is shown in Figure 5. This analysis would reveal contemporaneous relationships between RCs and tropical SST anomalies if any existed in the model. Figure 4 shows that the correlations are relatively strong for RCs 1, 3 and 4. The correlation between RC-1 and SSTs undoubtedly reveal an ENSO pattern with negative correlation over the tropical Pacific and positive correlations north and south (signs are arbitrary because of PCs). RC-3 has good correlation in the Indian Ocean as well as in the south Pacific between 150°E and 140°W. The dipole-like structure seen in the spatial EOF of RC-3 (Figure 4) and in the point correlation pattern (Figure 5) suggests its potential influence by the Indian Ocean dipole pattern seen in observations. The RC-4 is also largely influenced by the SST anomalies in the entire tropical belt. The pattern of correlations of RC-4 in the Pacific is very similar to that of RC-1 and is suggestive of an ENSO influence. However RC-4 has stronger correlation in the Indian Ocean compared to RC-1. The correlation patterns of RCs 2, 5 6 and 7 are more local in nature and their magnitudes are smaller compared to that of the RCs 1, 2 and 4. It appears that RC-8 has some amount of dependence on the SST anomalies both in the Indian Ocean and in the Pacific. The relatively weak dependence of

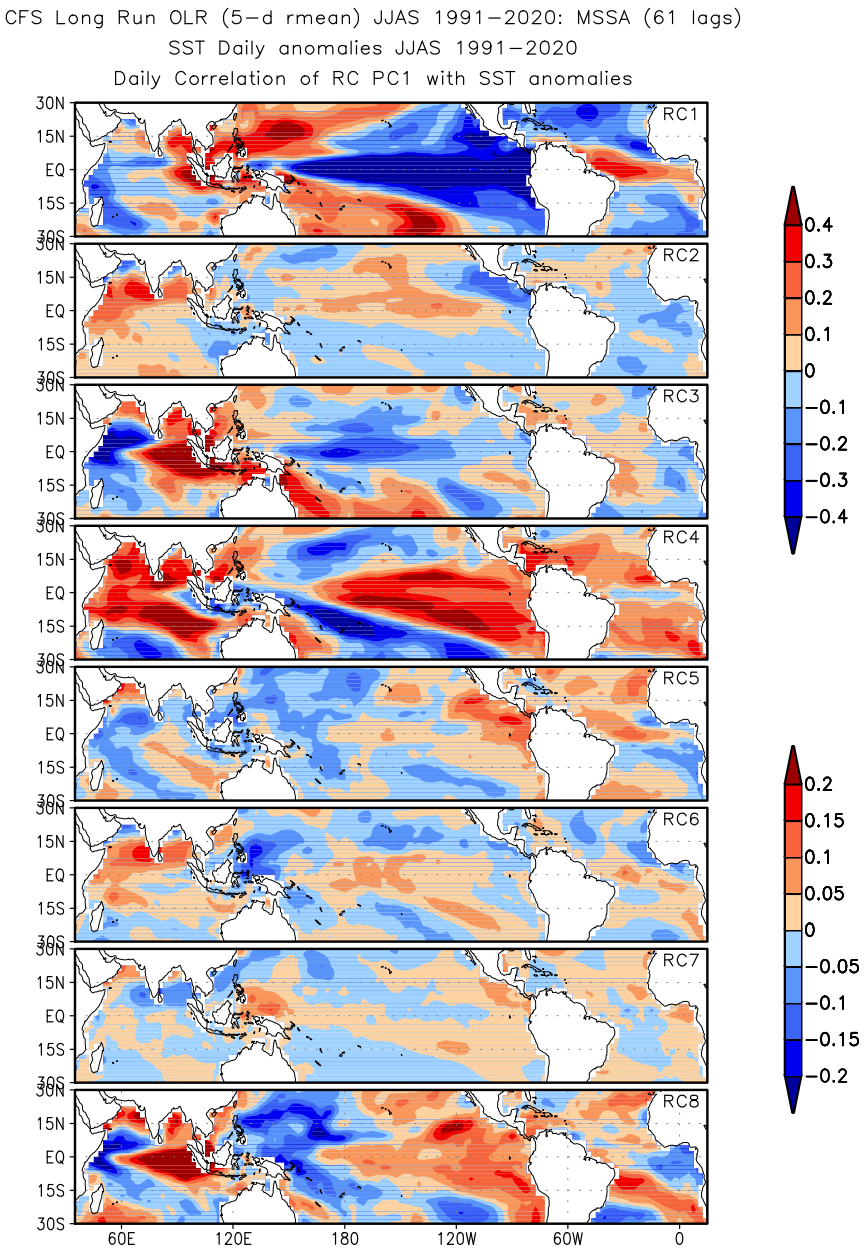

Figure 5. Daily point correlation between PC-1 of the spatial EOF-1 of the RCs and JJAS daily anomalies of SST. The top color bar applies to RCs 1 to 4 and the bottom one to RCs 5 to 8.

RCs 6 and 7 on SST anomalies suggests that these modes are likely to be more influenced by the atmospheric internal dynamics than by the boundary conditions. This is in agreement with the conceptual model proposed by KS00 and the MSSA results obtained from observations by KS06a and KS06b. The fact that RCs 2 and 5 also do not show strong correlations with SST leads us to speculate that these modes represent oscillations of subseasonal scale. It is possible that RCs 2 and 5 represent an equivalent of the 45-day oscillation found in observations but with longer period, and therefore, they are not properly resolved in the 61-day lag window used in this analysis. Further analysis is required to understand why the model does not show 45-day oscillations and whether RCs 2 and 5 suggest the presence of an oscillatory pair of longer perod.

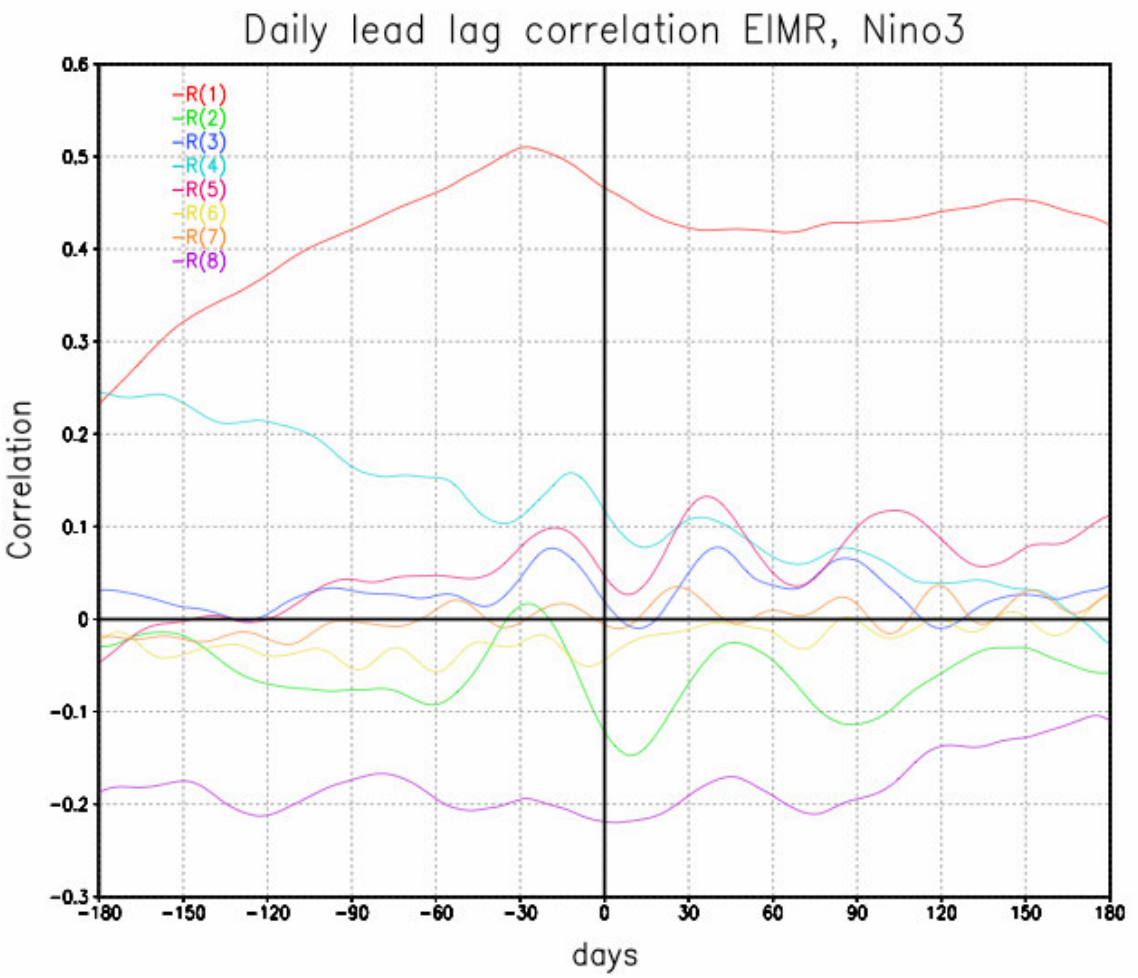

Figure 6. Daily lead lag correlation between (-) RCs averaged over the EIMR region and daily anomalies of Niño-3 index. The left side of the zero line refer to the period where Niño-3 leads monsoon and the right side refers to the period where Niño-3 lags monsoon.

anomalies are also examined. Daily correlations between RCs area averaged over the EIMR region and daily anomalies of NINO3 index (SST anomalies averaged over the Pacific Ocean region 150°W-90°W, 5°S-5°N) are computed. The correlations are found for a period of 361 days during which NINO3 leads monsoon and lags monsoon for up to 180 days each (Figure 6). RC-1 has the highest correlation with NINO3 on a daily basis. The correlation is around 0.2 about 6 months before the monsoon, gradually increases to 0.5 at lag -30 days, drops down slightly just after the monsoon season and stays above 0.4 for rest of the period. This reasonably good correlation between RC-1 and Niño-3 again suggests possible influence of ENSO on this particular mode. Consistent with the simultaneous correlation calculations (Figure 4), the dependence of oscillatory modes (RCs 6 and 7) on SST anomalies is rather weak. However we note a slight increase in the correlation values for almost all RCs just before the monsoon as well as a slight decrease just after the season. It is unclear whether this can be linked to any possible but weak influence of ENSO on all the modes.

6. SUMMARY

This study has investigated the subseasonal oscillations of the summer monsoon and their relation with the interannual variability in a coupled GCM by analyzing a 30-year long daily precipitation and OLR data from the simulation by CFS, the latest coupled GCM developed by the NCEP. The spatial patterns of daily and seasonal variability were examined using composite and pattern correlation techniques. The composites of

active and break phases and strong and weak monsoon years do not show a clear difference in spatial patterns unlike the observational results by KS00. However the pattern correlations between daily and seasonal anomalies of rainfall suggest the existence of a seasonally persistent component. It is unclear why the results of the composite analysis are not consistent with those of observations.

The dominant modes of subseasonal variability and their propagation in time were examined by applying MSSA on daily anomalies of OLR data. The MSSA reveals three seasonally persisting modes and one oscillatory mode. The oscillatory component is found to be of 30-day period and seems to be the equivalent of the 28-day mode obtained in observations. However, the spatial features and propagation characteristics of this mode do not compare well with the observations. One of the important results from the MSSA is that the 45-day oscillation found in observations that provides most of the northward and eastward propagation as well as in-situ expansion during an active-break cycle is absent in the model. However we observe two separate eigenmodes that are not resolved as an oscillatory pair but contain signatures of oscillations in longer time scales. It is possible that the equivalent of 45-day oscillation in the model is of longer period and is not properly resolved in the 60-day lag window used in this study. The spatial structure of the three seasonally persistent components appears to carry signatures of ENSO and Indian Ocean dipole patterns. The most dominant seasonally persistent ENSO signal explains most of the interannual variability in the model. The seasonal means of the oscillatory components are found to be close to zero. The seasonally persistent signals were found to have good correlation with SST while the oscillatory pair appears to be less dependent on the boundary conditions. This result is consistent with the conceptual model proposed by KS00 and brings hope for seasonal prediction of monsoon. It is also found that the dominant persistent signal has a reasonably good correlation with NINO3 SST on a daily basis, which also provides hope for predictability.

7. REFERENCES

Charney, J. G., and J. Shukla, 1981: Predictability of monsoons. *Monsoon Dynamics*, J. Lighthill and R. P. Pearce, eds., Cambridge University press, 99-109.

Ghil, M., M. R. Allen, M. D. Dettinger, K. Ide, D. Kondrashov, M. E. Mann, A. W. Robertson, A. Saunders, Y. Tian, F. Varadi and P. Yiou, 2002: *Rev. Geophys.*, **40(1),** 1003, doi:10.1029/2000RG000092.

Goswami, B. N., V. Krishnamurthy and H. Annamalai, 1999: A broad-scale circulation index for the interannual variability of the Indian summer monsoon. *Quart. J. Roy. Meteor. Soc.*, **125,** 611-633.

Krishnamurthy, V., and J. Shukla, 2000: Intraseasonal and interannual variability over India. *J. Climate*, **13,** 4366 – 4377.

Krishnamurthy, V., and J. Shukla, 2006a: Intraseasonal and Seasonally Persisting Patterns of Indian Monsoon Rainfall. *J. Climate* (in press).

Krishnamurthy, V., and J. Shukla, 2006b: Seasonal persistence and propagation of intraseasonal patterns over the Indian monsoon region. *Clim. Dyn*. (in review).

Palmer, T. N., 1994: Chaos and predictability in forecasting the monsoons. *Proc. Indian natl. Sci. Acad.*, **60A,** 57-66.

Plaut, G., and R. Vautard, 1994: Spells of low-frequency oscillations and weather regimes in the Northern Hemisphere. *J. Atmos. Sci.*, **51,** 210-236

S. Saha, S. Nadiga, C. Thiaw, J. Wang, W. Wang, Q. Zhang, H. M. van den Dool, H.-L. Pan, S. Moorthi, D. Behringer, D. Stokes, M. Pena, S. Lord, G. White, W. Ebisuzaki, P. Peng, P. Xie , 2006: The NCEP Climate Forecast System. *J. Climate*, **19,** 3483 – 3517.